From: STIC-ILL
Sent: Wednesday, September 25, 2002 2:31 PM
To: Jacob, Rebecca (ASRC)
Subject: RE: ILL order

01/8255Y)

8/31/00

-----Original Message-----
From: Bates, Darcy
Sent: Wednesday, September 25, 2002 2:26 PM
To: STIC-ILL
Cc: Harrison, Jeff; Blalock, Derrick (ASRC); Speckhard, Irina (ASRC); Amari, Alessandro
Subject: ILL order

Hi,

We do not have the following item in STIC. Please order this item for Alessandro Amari, CP4-7A07.

ILL Ordering Information

Date Needed<9-27-02>

Art Unit or Location <2872>

Telephone Number <306-0533>

```
Title: On    transition    temperatures    in    the    plasticity   and  fracture   of
semiconductors.
Author(s): Pirouz-P; Demenet-J-L; Hong-M-H.
IN Dept  of  Mater  Sci  & Eng, Case Western Reserve Univ, Cleveland, OH,
   USA.
Source: Philosophical-Magazine-A  (Physics  of  Condensed  Matter:  Structure,
   Defects  and  Mechanical  Properties)(UK),  vol.81,  no.5,  p.1207-27, May
   2001. , Published: Taylor & Francis.
CD PMAADG.
RN ISSN: 0141-8610.
CP Copyright 2001, IEE.
DO http://dx.doi.org/10.1080/01418610110033939.
DB INZZ - INSPEC ENGINEERING '69-V2002:I38

Thank you,
```

Darcy Bates
EIC 2800 Technical Information Specialist
U.S. Patent & Trademark Office
(703)306-5419   Email: STIC-EIC2800
dbates@uspto.gov

9/26

UHL

Status 10/9

1

On transition temperatures in the plasticity and fracture of semiconductors

P. PIROUZ†§, J. L. DEMENET‡ and M. H. HONG†

† Department of Materials Science and Engineering, Case Western Reserve University, Cleveland, Ohio 44106-7204, USA

‡ Laboratoire de Métallurgique Physique (Unité Mixte de Recherche associée au CNRS 630), SP2MI, Université de Poitiers, BP 179, 86960 Futuroscope Cedex, France

ABSTRACT

Recent experiments on deformation of semiconductors show an abrupt change in the variation in the critical resolved shear stress τ_Y with temperature T. This implies a change in the deformation mechanism at a critical temperature T_c. In the cases examined so far in our laboratories (Case Western Reserve University and Poitiers) and elsewhere, this critical temperature appears to coincide approximately with the brittle-to-ductile transition temperature T_{BDT}. In this paper, new deformation experiments performed on the wide-bandgap semiconductor 4H-SiC over a range of temperatures at two strain rates are described together with a transmission electron microscopy characterization of induced dislocations below and above T_c. Based on these, and results recently reported on a few III–V compound semiconductors, a new model for the deformation of tetrahedrally coordinated materials at low and high temperatures is proposed, and the relation of the transition in deformation mode to the transition in fracture mode (brittle to ductile) is discussed.

§1. INTRODUCTION

The plasticity and fracture of semiconductors have interested materials scientists for a long time because, compared with possibly any other material, semiconductors can be grown as crystals of exceptionally high quality. In particular, since the invention of the transistor in 1949, techniques have been developed to grow many semiconducting crystals to contain a very low density of dislocations (or none in the case of silicon) or, for that matter, any other type of defect. Consequently, cracks or dislocations can be introduced in an initially defect-free (or nearly so) material in a controlled manner and their behaviour studied under the application of a tensile or shear stress.

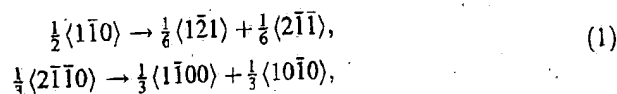### 1.1. Plastic properties of semiconductors

Some of the early work on the plasticity of semiconductors was carried out by Alexander, Haasen and their co-workers and was reviewed in their seminal paper (Alexander and Haasen 1968). More recent reviews of the work in this area are by

§ Email: pxp7@cwru.edu

1208

Alexander (1986), and by George and Rabier (1987) and Rabier and George (1987). The topics reviewed in these papers deal with macroscopic plastic properties of semiconductors, such as their upper and lower yield stresses as functions of deformation temperature and strain rate, as well as with microscopic mechanisms of yielding involving dislocation glide. From both macroscopic and microscopic measurements of plastic properties, the activation parameters of dislocation glide can be determined. Before reviewing these, however, we shall briefly discuss the structure and dynamics of dislocations in tetrahedrally coordinated materials.

1.2. *Dislocations in tetrahedrally coordinated materials*

Dislocations in tetrahedrally coordinated materials glide most easily on the $\{111\}$ slip planes in cubic crystals and the (0001) slip planes in hexagonal materials and have Burgers vectors $\mathbf{b} = \frac{1}{2}\langle 1\bar{1}0 \rangle$ in the former and $\mathbf{b} = \frac{1}{3}\langle 11\bar{2}0 \rangle$ in the latter. Because of the high Peierls potential in such crystals, the dislocations lie in the Peierls valleys that are parallel to $\langle 1\bar{1}0 \rangle$ in cubic crystals and $\langle 11\bar{2}0 \rangle$ in hexagonal crystals. As a result an ideal dislocation loop has a hexagonal shape with the segments parallel to the Peierls valleys, that is all the segments are 60° or screw dislocations. In all the tetrahedrally coordinated materials that have been studied to date, the dislocations are dissociated according to the following reactions:

$$\tfrac{1}{2}\langle 1\bar{1}0 \rangle \rightarrow \tfrac{1}{6}\langle 1\bar{2}1 \rangle + \tfrac{1}{6}\langle 2\bar{1}\bar{1} \rangle, \tag{1}$$

$$\tfrac{1}{3}\langle 2\bar{1}\bar{1}0 \rangle \rightarrow \tfrac{1}{3}\langle 1\bar{1}00 \rangle + \tfrac{1}{3}\langle 10\bar{1}0 \rangle,$$

that is the partials are either 90° or 30° dislocations. The separation of the partials is of course determined by the stacking fault energy γ of the material. The latter ranges from about $2.5\,\mathrm{mJ\,m^{-2}}$ in SiC to about $280\,\mathrm{mJ\,m^{-2}}$ in diamond (Gottschalk *et al.* 1978, Takeuchi *et al.* 1984, Takeuchi and Suzuki 1999). In addition, in the case of compound semiconductors, the core of all the dislocations consists of only one atom species (see for example Pirouz and Ning (1995)). Thus, an idealized dissociated dislocation loop of, say, hexagonal SiC will have the configuration shown in figure 1; depending on expansion or contraction, the outer and inner loops correspond to the leading and trailing partials respectively. Note that a 60° dislocation dissociates into a 90° and a 30° partial where both of the partials have the *same* core (either both Si(g) or both C(g) using the notation of Alexander *et al.* (1979)). On the other hand, a screw dislocation dissociates into two 30° partials that have *different* core structures (e.g. one is Si(g) while the other is C(g)). Also note that half the segments in both the inner and the outer loops have a silicon core while the segments in the other half have a carbon core (i.e. one can envisage *half-loops* that have a completely silicon or a completely carbon core). We shall later argue that the core nature of the different partials in such dislocation loops plays a significant role in the mode of deformation that occurs in tetrahedrally coordinated materials.

1.3. *Dynamics of dislocation glide*

In general, the dislocation velocity v in a tetrahedrally coordinated material can be expressed in the following form:

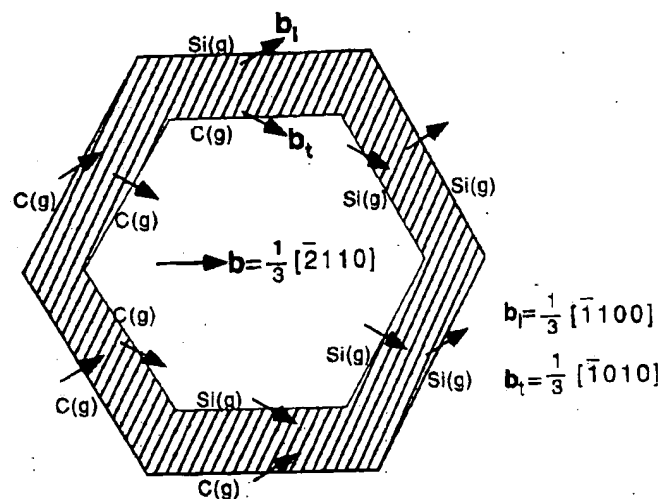$$v = v_0 \exp\left(-\frac{\Delta G_\tau^T(\tau, T)}{kT}\right), \tag{2}$$

Figure 1. A dissociated hexagonal loop on the (0001) slip plane in SiC.

where the stress τ and temperature T dependence of the dislocation velocity are incorporated in the free-energy barrier $\Delta G(\tau, T)$ for dislocation motion. In the absence of applied stress ($\tau = 0$), the free-energy barrier $\Delta G_0^T = \Delta G(0, T)$ is assumed to have the same temperature dependence as the shear modulus μ. In many cases, over a large range of stresses and temperatures, the dislocation velocity can be expressed in terms of the following phenomenological equation:

$$v = A \left(\frac{\tau}{\tau_0} \right)^m \exp\left(-\frac{\Delta H_g}{kT} \right), \qquad (3)$$

where ΔH_g is a stress- and temperature-independent activation enthalpy change for dislocation glide, and A, τ_0 and the stress exponent m are constants (A includes an activation entropy term for dislocation glide and $\tau_0 = 1$ MPa if τ is in megapascals). In this form, the stress dependence of the dislocation velocity appears in the pre-exponent and the activation enthalpy is assumed to be a constant ΔH_g.

The relation between macroscopic and microscopic plastic properties of a crystal are given by Orowan's equation for the plastic strain rate $\dot{\gamma}$:

$$\dot{\gamma} = \rho b v, \qquad (4)$$

where ρ is the density of mobile dislocations and b is the magnitude of the Burgers vector of dislocations producing the shear strain γ. Thus, combining equations (4) and (2), one has

$$\dot{\gamma} = \rho b v_0 \exp\left(-\frac{\Delta G_\tau(\tau, T)}{kT} \right). \qquad (5)$$

In this case, the stress dependence of $\Delta G_\tau = \Delta H_\tau - T \Delta S_\tau$ (where ΔH_τ and ΔS_τ are the enthalpy and entropy changes, respectively) can be determined from the activation volume, $V^* = -(\partial G_\tau / \partial \tau)_T = -(\partial H_\tau / \partial \tau)_T$, using stress relaxation tests or strain-rate jump tests (for example Kubin (1974), Kocks *et al.* (1975)).

If equation (3) is applicable in the range of stresses and temperatures under consideration, then one can determine the stress-independent activation enthalpy ΔH_g and the stress exponent m from a direct measurement of dislocation velocity as a function of temperature and applied stress. A different way to determine the activation parameters of dislocation glide involves measurement of the yield stress τ_Y as a function of temperature and applied stress. This is again obtained by combining the macroscopic parameters of yield and microscopic properties of dislocation through substituting equation (3) for dislocation velocity in Orowan's relation (4) to give (Alexander and Haasen 1968)

$$\tau_Y = \dot{\gamma}^{1/n} \exp\left(\frac{Q}{kT}\right). \tag{6}$$

Thus, it is possible to determine the constant Q by measuring the critical resolved shear stress as a function of temperature at a fixed strain rate. In addition, the constant n can be determined by performing strain-rate jump tests (for example Samant and Pirouz (1998)). The constants n and Q are related to the phenomenological parameters m and ΔH_g describing the dislocation velocity in equation (3). The relation between the constants n and m, and ΔH_g and Q can be derived from the kink diffusion model of dislocation glide as $n = m + 2$ and $\Delta H_g = nQ$ (for example Alexander and Haasen (1968)).

The facts that dislocations in semiconductors are straight when produced at low temperatures and lie along the $\langle 110 \rangle$ directions are highly suggestive that their motion is controlled by a high Peierls stress and that, at finite temperatures, they move by the mechanism of kink pair formation and kink migration. Employing the kink diffusion model of Hirth and Lothe (1968), the activation enthalpy ΔH_g can be related to the enthalpy ΔH_{kf} required for kink pair formation and the enthalpy ΔH_{km} required for kink migration. Although, formerly, it was thought that, just as in fcc crystals, the kink migration energy is rather negligible and $\Delta H_g \approx \Delta H_{kf}$, this assumption has recently been questioned and the kink migration energy in tetrahedrally coordinated materials may turn out to be large and even $\Delta H_{km} \geq \Delta H_{kf}$. For details of measuring ΔH_g, ΔH_{kf} and ΔH_{km}, reference can be made to the aforementioned review papers of George and Rabier (1987) and Rabier and George (1987).

1.4. *Fracture behaviour of semiconductors*

The work on the fracture of semiconductors started much later than the work on the plasticity of these materials. At low temperatures, semiconductors are brittle materials; the *elemental* semiconductors (silicon, germanium and diamond) cleave preferentially on a {111} plane whereas the (cubic) *compound* semiconductors preferentially cleave on a {110} plane (similarly the hexagonal semiconductors cleave on a {10$\bar{1}$0} plane). One of the earliest papers on fracture of semiconductors reported measurement of the surface energy of {111} planes in silicon by cleavage (Gilman 1960). However, the first systematic fracture study of a semiconductor was made by St John (1975) who performed careful fracture measurements at different strain rates on pre-cracked silicon single crystals over a wide range of temperatures (between -196 and 1000°C). He found a very narrow temperature range (a few degrees Celsius) over which silicon changed from a brittle to a ductile behaviour. This brittle-to-ductile transition (BDT) temperature T_{BDT} was found to be a sensitive function of the applied strain rate $\dot{\varepsilon}$ (or, equivalently, the rate $\dot{K}$ of application of

res under
enthalpy
n velocity
rmine the
l stress τ_Y
ombining
islocation
lation (4)

(6)

resolved
tion, the
example
nomeno-
ttion (3).
from the
example

:d at low
nat their
res, they
ying the
Γ_g can be
:nthalpy
hat, just
$\approx \Delta H_{kf}$,
iergy in
d even
: can be
l Rabier

vork on
: brittle
) cleave
)rs pre-
:ave on
:ported
Gilman
iade by
in rates
:tween
legrees
:. This
insitive
tion of

the stress intensity factor K) and was thermally activated with an activation energy close to that for dislocation glide. The seminal work of St John on silicon was later repeated and extended by a number of researchers including extensive studies by Brede and Haasen (1988), Michot (1988), Haasen *et al.* (1989), Hirsch *et al.* (1989a,b), Hirsch and Roberts (1991), Hsiah and Argon (1994), George (1998). These researchers extended the work of St John to include the influence of various variables on the BDT temperature, such as electrically inactive impurities (e.g. oxygen and hydrogen), electrically active dopants (e.g. donors and acceptors) and crack plane orientation. Tests were also conducted on a few other semiconductors such as germanium (Serbena and Roberts 1994), GaAs (Michot *et al.* 1988, Michot and George 1989) and SiC (Maeda and Fujita 1989). Most of the experiments mentioned have been performed at a constant rate $\dot{K}$ of increase in the stress intensity factor K under a mode I loading geometry. In this mode, the tensile stress σ is applied perpendicular to the crack plane (see, for example figure 10 later). The microscopic studies of the fractured samples, by X-ray topography (Michot and George 1982, 1986, George and Michot 1993) or by transmission electron microscopy (TEM) (Chiao and Clarke 1989), have shown that there is hardly any dislocation activity below T_{BDT}, while an avalanche of dislocations nucleate at this critical temperature.

The most quantitative model proposed for the BDT in silicon is by Hirsch and Roberts (1991) where the shielding of the crack front by dislocations emitted from there competes with the rise in the stress intensity factor K to the critical value K_{Ic}. The dislocations are assumed to be emitted from a few special sites along the crack tip; these primary sites are separated from each other by an average distance d_1. Subsequently, the loops emitted from these sites help to activate nucleation from other, more difficult sites along the crack front. These secondary sites are separated from the primary sites by an average distance d_2 (usually taken to be equal to $d_1/2$). The main feature of the model is that it is only when the emitted dislocations shield *every* point of the crack front that the material becomes ductile and the crack front is not able to propagate catastrophically. Under a constant $\dot{K}$, with an increasing K, the shielding is considered to be effective if the dislocation loops expand at a sufficiently rapid rate that they cover the whole of the crack front before K reaches K_{Ic}. In this sense, the mobility of dislocations plays the major role in the Hirsch–Roberts model because the loops from the primary sources must traverse a distance $d_1 - d_2$ to cover every point on the crack before K increases to the critical value K_{Ic}. The distances d_1 and d_2, as well as the stress intensity factors K_1 and K_2, required to nucleate dislocation loops at the primary and secondary sites respectively are used as fitting parameters in the model. With the help of these four fitting parameters, reasonably good agreement with experimental results have been obtained for the prediction of T_{BDT} as well as for the variation in T_{BDT} with $\dot{K}$; for more detail, refer to the original papers of Hirsch and Roberts (1991, 1997).

The Hirsch–Roberts model has recently been criticized by Khanta (1994) and Khanta *et al.* (1994a,b) on the grounds that a thermally activated process cannot explain the sharpness of T_{BDT} (see, however, the series of correspondence between Hirsch and Roberts (1996a,b) and Khanta and Vitek (1996)). In analogy with the Kosterlitz–Thouless (1973) model of paraelectric-to-ferroelectric transition, Khanta *et al.* have proposed a model based on autocatalytic nucleation of dislocations in the material at T_{BDT} (see also Sun *et al.* (1998)). As will be seen below, the sharpness of

P. Pirouz *et al.*

the BDT temperature in our model arises from the nucleation of an avalanche of *trailing* partial dislocations under the applied stress aided by thermal activation.

1.5. *Plasticity of semiconductors in the brittle regime*

Many interesting experiments on the yield behaviour of semiconductors involve deformation at low temperatures where the crystals are usually brittle. A number of such experiments have been performed by Vickers indentation where the indentation stress field has a hydrostatic component that prevents the fracture of the material. Superimposed on this hydrostatic component, there are large tensile or compressive and shear stresses that plastically deform the material by shear (for example, Hirsch *et al.* (1985)). However, it is not usually possible to obtain quantitative data on the yield stress and dislocation glide activation parameters from indentation tests. Thus, the more useful low-temperature deformation experiments involve uniaxial tests such as tension or compression. One way to perform such tests is to pre-deform the material at a high temperature (in the ductile regime) and subsequentialy to deform it (usually by compression) at a lower temperature (in the brittle regime) (for example Wessel and Alexander (1977)). It should be mentioned that, if the initial dislocation density in the material is sufficiently high, a pre-deformation is not essential and, as long as the deformation is performed in a carefully aligned compression jig under very low stram rates, it is possible to deform the sample plastically at temperatures down to a few hundred degrees celsius below the BDT. A different technique for low-temperature deformation is to perform the compression (or even tensile) test in the presence of a superimposed hydrostatic pressure in order to prevent the fracture of the test sample. An early study in this respect was that of Castaing *et al.* (1981) who deformed silicon in the temperature range 300–600°C in a Griggs apparatus, usually used for deformation of brittle geological materials. Rabier *et al.* (1985), Demenet (1987) and Demenet *et al.* (1989) later performed similar types of experiments on silicon and on GaAs. More recently, Suzuki *et al.* (1998, 1999a,b) and Edagawa *et al.* (2000) used a similar technique to deform InP, InSb, GaAs, and GaP; as before, the hydrostatic pressure prevented fracture of the deformation samples before they plastically yielded.

In our laboratories (Case Western Reserve University (CWRU) and Laboratoire de Métallurgique Physique (LMP)), research has concentrated on two different hexagonal polytypes of the wide-bandgap semiconductor SiC. As part of his PhD thesis, Samant (1999) investigated the plastic behaviour of 4H-SiC and 6H-SiC by compression tests over a wide range of temperatures and strain rates. It should be mentioned that, because single crystals of these two semiconductors were not available until recently, prior to the work of Samant, there were only a few reports of deformation tests on single-crystal 6H-SiC and almost none on 4H-SiC. Some important studies that existed were compression temperature range by Fujita *et al.* (1987) on Acheson-grown 6H-SiC crystals over the temperature range 1300–1600°C, and creep tests on Cree-grown 6H-SiC by Corman (1992). Samant's experiments covered the temperature range 550–1400°C at strain rates varying from 6.5×10^{-4} to $3.1 \times 10^{-5}\,\mathrm{s}^{-1}$. He was able to deform the crystals at temperatures below their usual range of BDT because of the rather high initial density of dislocations in the samples (about 10^{3}–$10^{4}\,\mathrm{cm}^{-2}$), careful alignment of the sample in the deformation jig and with the use of very low strain rates (Samanz and Pirouz 1998, Samant *et al.* 1998, Samant 1999). More recently, Demenet *et al.* (2000) repeated Samant's experiments on 4H-SiC (grown at Cree Research, Inc.) obtaining much more data in the temperature

range 900–1360°C at both CWRU and LMP. Here we report some of the experimental measurements of Demenet *et al.* and discuss their implications for the plasticity and fracture of semiconductors.

§2. Yield behaviour of 4H-SiC single crystals

2.1. *Experimental procedures*

The details of the experimental procedure for deforming the SiC crystals have been given elsewhere (Samant 1999). Briefly, a single-crystal ingot of 4H-SiC grown at Cree Research, Inc., was oriented for single glide (Schmid factor $S = 0.5$) on one of the three primary slip systems $\langle 11\bar{2}0\rangle(0001)$ using X-ray diffraction. From the ingot, $2.2\,\text{mm} \times 2.2\,\text{mm} \times 4.7\,\text{mm}$ samples were cut and carefully polished on all faces. The compression tests were made over the temperature range 800–1360°C using two strain rates varying by an order of magnitude ($\dot{\varepsilon} \approx 3.6 \times 10^{-5}$ and $2.6 \times 10^{-6}\,\text{s}^{-1}$). The series of deformation tests at a strain rate of $\dot{\varepsilon} \approx 3.6 \times 10^{-5}\,\text{s}^{-1}$ were performed at CWRU, while those at a strain rate of $\dot{\varepsilon} \approx 2.6 \times 10^{-6}\,\text{s}^{-1}$ were performed at LPM; no hydrostatic confining pressure was used in any of these tests. It should also be mentioned that tests in the latter laboratory using $\dot{\varepsilon} \approx 3.6 \times 10^{-5}\,\text{s}^{-1}$ basically reproduced the results obtained earlier at CWRU (for more details, see Demenet *et al.* (2000)). Following the mechanical tests, thin foils parallel to the (0001) slip planes were prepared from the samples deformed at temperatures above and below the transition temperature. In addition to strain contrast experiments to characterize the Burgers vectors of the dislocations, the large-angle convergent-beam electron diffraction (LACBED) technique (Cherns and Preston 1986, Chou *et al.* 1992) was used to identify the nature of dislocation cores (Ning and Pirouz 1996).

2.2. *Results*

Figure 2 shows a plot of $\ln(\tau_Y)$ versus $1/T$ for two strain rates: $\dot{\varepsilon} \approx 3.6 \times 10^{-5}$ and $2.6 \times 10^{-6}\,\text{s}^{-1}$. As in the previous experiments on 4H- and 6H-SiC (Samant and Pirouz 1998, Samant *et al.* 1998, Samant 1999), there is a sharp transition at a critical temperature T_c. A significant point about these curves is the shift of T_c to a lower temperature as the strain rate is lowered. Thus, whereas $T_c \approx 1100°C$ for $\dot{\varepsilon} \approx 3.6 \times 10^{-5}\,\text{s}^{-1}$, the transition temperature is shifted by 70°C to a lower temperature of $T_c \approx 1030°C$ when the slower strain rate $\dot{\varepsilon} \approx 2.6 \times 10^{-6}\,\text{s}^{-1}$ is used. It should be noted that, while macroscopic plastic deformation of 4H-SiC (and 6H-SiC) is relatively easy at $T > T_c$, it becomes very limited at $T < T_c$ and, when the samples have not failed catastrophically, deformation is very often accompanied by the appearance of extensive microcracking. These observations, from a fully plastic crystal with no evidence of any cracking when deformed at $T > T_c$ to a crystal that undergoes very limited plasticity accompanied by profuse microcracking when deformed at $T < T_c$, indicate that the BDT temperature of 4H-SiC is very close to T_c. This is also consistent with the experiments of Fujita *et al.* (1987) and Maeda and Fujita (1989) on 6H-SiC who concluded that the BDT temperature of this material is above 800–1000°C. The activation enthalpy Q (see equation (6)) was determined from the slopes of the straight lines in figure 2 and found to be about 1.7 eV (in the $T > T_c$ regime). Using a value of $n \approx 3$, determined on a different 4H-SiC sample by Samant and Pirouz (1998) and Samant (1999), and also a few strain-rate jump tests on the new 4H-SiC material by Demenet *et al.* (2000), gives

P. Pirouz *et al.*

Figure 2.   Plot of $\ln(\tau_Y)$ versus $1/T$ for 4H-SiC deformed at strain rates of $3.6 \times 10^{-5}\,\text{s}^{-1}$ (O) and $2.6 \times 10^{-6}\,\text{s}^{-1}$ (●).

$Q \approx 1.5$ and $1.8\,\text{eV}$ at $\dot{\varepsilon} \approx 3.6 \times 10^{-5}$ and $2.6 \times 10^{-6}\,\text{s}^{-1}$ respectively, resulting in $\Delta H_g \approx 4.5 \times 0.3\,\text{eV}$ for the former strain rate $\Delta H_g \approx 5.1 \pm 0.3\,\text{eV}$ for the latter strain rate.

Following the compression experiments, extensive TEM of the deformed samples was performed. In figure 3, the dislocation configurations in two of the samples deformed at a temperature higher than T_c are shown: figures 3 (*a*) and (*b*) correspond to deformation at $T = 1200°\text{C}$ and $\dot{\varepsilon} \approx 3.6 \times 10^{-5}\,\text{s}^{-1}$, whereas figures 3 (*c*) and (*d*) correspond to deformation at $T = 1280°\text{C}$ and $\dot{\varepsilon} \approx 2.6 \times 10^{-6}\,\text{s}^{-1}$ These are representative of the microstructure of many samples deformed at $T > T_c$ for both strain rates and show that deformation of 4H-SiC above the transition temperature generates a large density of $\mathbf{b} = \frac{1}{3}\langle11\bar{2}0\rangle$ dislocations dissociated into $\frac{1}{3}\langle10\bar{1}0\rangle$ leading–trailing partial pairs on the (0001) slip plane. It is also noteworthy that a Burgers vector analysis reveals that most of the dislocations have a screw character, presumably indicating that the mobility of non-screw dislocations is higher in this material, something that is consistent with other tetrahedrally coordinated materials. In contrast with the samples deformed at $T > T_c$, there is a very low density of dislocations generated by deformation at $T < T_c$ and these are predominantly 30° single leading partials all with the same Burgers vector $\mathbf{b}_l = \frac{1}{3}\langle10\bar{1}0\rangle$. Examples of these are shown in figures 4 and 5 for deformations at $T = 1000$ and $840°\text{C}$ at the higher $(\dot{\varepsilon} \approx 3.6 \times 10^{-5}\,\text{s}^{-1})$ and lower $(\dot{\varepsilon} \approx 2.6 \times 10^{-6}\,\text{s}^{-1})$ strain rates respectively. Figures 4 (*a*) and 5 (*a*) show the dislocation configurations on the (0001) slip planes; with the reflection $\mathbf{g} = 11\bar{2}0$ used for imaging, the stacking faults behind the partials are out of contrast. On the other hand, in figures 4 (*b*) and 5 (*b*), the reflection $\mathbf{g} = 1\bar{1}01$ is used to show the stacking-fault contrast. The appearance of overlapping stacking faults indicates that the leading partials are on parallel slip planes. In addition to the strain contrast experiments, the cores of a number of single partial dislocations, produced by deformation at temperatures below T_c, were identified by the technique of LACBED. Examples of LACBED patterns for one of the dislocations in figures 4 (*a*) and 5 (*a*) are shown in figures 4 (*c*) and 5 (*c*), respectively; in all cases examined, the core of the leading partial has turned out to be silicon rather than carbon.

Figure 3. Transmission electron micrographs of dissociated total dislocations in 4H-SiC showing (*a*), (*c*) leading–trailing partial dislocation pairs and (*b*), (*d*) stacking-fault contrast for deformation at (*a*), (*b*) $T = 1200°C$ and $\dot{\varepsilon} \approx 3.6 \times 10^{-5}\,s^{-1}$ and (*c*), (*d*) 1280°C and $\dot{\varepsilon} \approx 2.6 \times 10^{-6}\,s^{-1}$.

Figure 4. (*a*) Bright-field micrograph of dislocations in 4H-SiC deformed at $T = 1000°C$ and $\dot{\varepsilon} \approx 3.6 \times 10^{-5}\,s^{-1}$ showing single leading partial dislocations; (*b*) same region as (*a*) showing overlapping stacking faults; (*c*) a LACBED pattern of a single leading partial in (*a*).

Left margin fragments:
s^{-1} (○)

lting in
e latter

amples
amples
espond
and (*d*)
repre-
strain
re gen-
ading–
Burgers
resum-
aterial,
n con-
cations
eading
shown
higher
igures
ith the
re out
$\bar{1}01$ is
icking
to the
itions,
unique
igures
nined,
1.

P. Pirouz *et al.*

1216
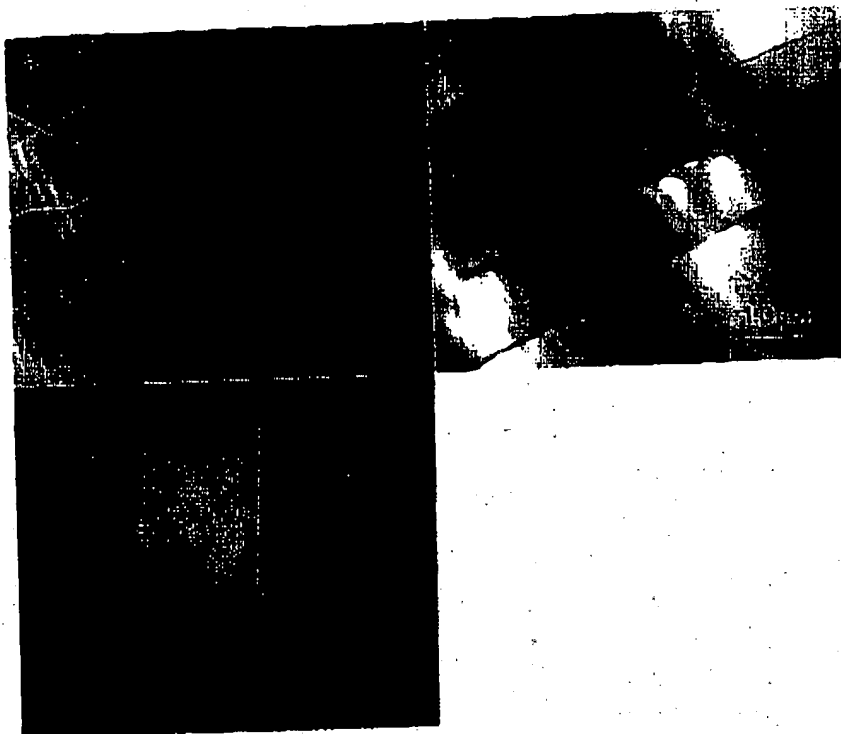
Figure 5. (*a*) Bright-field micrograph of dislocations in 4H-SiC deformed at $T = 840°C$ and $\dot{\varepsilon} \approx 2.6 \times 10^{-6} \, s^{-1}$, showing single leading partial dislocations; (*b*) same region as (*a*) showing overlapping stacking faults; (*c*) a LACBED pattern of a single leading partial in (*a*).

§3. Discussion

Similar to figure 2, plots of the critical yield stress versus temperature for all the other five compound semiconductors mentioned previously (InSb, InP, GaAs (Suzuki *et al.* 1999b), GaP (Edagawa *et al.* 2000) and 6H-SiC (Samant and Pirouz 1998)) show an abrupt transition at a critical temperature T_c. It is possible that this transition exists in all the tetrahedrally coordinated materials and signifies a change in the deformation mode in the material. Also, intriguingly, in every case the transition temperature in the $\tau_Y(T)$ plot appears to coincide approximately with the BDT temperature T_{BDT} of that material, taking due account of the strain rate. Suzuki *et al.* (1999a,b) explained the change in the deformation mechanism at T_c in the compound semiconductors that they studied by a change in the slip plane (shuffle to glide) on which dislocations glide. Thus two regimes for dislocation motion in these materials were proposed: perfect screw dislocations moving in the shuffle set at low temperatures versus dissociated dislocations moving in the glide set at high temperatures. These arguments were based on some compelling experimental evidence including the observation of wavy slip lines on the surfaces of samples deformed at low temperatures (indicating cross-slip, something that is only possible for perfect screw dislocations), small activation volumes at low temperatures, and a temperature dependence of τ_Y that is more consistent with kink pair formation in perfect screw dislocations rather than in partial dislocations. The observation of dissociated dislocations by TEM in their low-temperature-deformed samples was attributed to post-mortem relaxation of stress and pressure after deformation. In this way they assumed that, although perfect screw dislocations are responsible for the deforma-

tion at
deform:
tempera
work o
Duesbe:
shuffle
stacking
1993), a
location
al. (199:
(1995) i:
shuffle (
tions on
at finite
dislocat.
by kink
enthalp:
very hig
nificantl
glide pl:
In tl
yield st:

As :
of the :
Si(g) le
sisted p
now co
rally cc
crystal
Howev
(by the
not be
the str
disloce
In
play a
energy
ΔH_n t
mally
a freq
overc(
activa

that
$t = (1$

tion at low temperatures, they dissociate into their equilibrium width after the deformation has stopped. The suggestions of Suzuki *et al.* (1999a,b) on the low-temperature motion of perfect dislocations in the shuffle plane is consistent with the work of Kaxiras and Duesbery (1993), Joós *et al.* (1994). Ren *et al.* (1995) and Duesbery and Joós (1996). Thus, Joós *et al.* (1994) calculated the Peierls stress for shuffle and glide dislocations using the Peierls–Nabarro model with generalized stacking faults, determined by density functional methods (Kaxiras and Duesbery 1993), and found values nearly an order of magnitude higher for glide partial dislocations than for shuffle dislocations. Comparative values were obtained by Ren *et al.* (1995) employing atomistic calculations based on the empirical Stillinger–Weber (1995) interatomic potentials. The conflict between theoretical predictions of perfect shuffle dislocations and experimental observation of exclusively dissociated dislocations on the glide plane was explained by Duesbery and Joós (1996) on the basis that, at finite temperatures, in silicon and related materials where there is significant dislocation–lattice coupling, dislocations do not move by rigid translation but rather by kink pair nucleation and migration. They then calculated the kink pair formation enthalpy using a quasistatic model (Hansen *et al.* 1995) and found that, except at very high stresses (above 1 GPa), the activation enthalpy for a (30°) partial is significantly lower than that for a shuffle screw dislocation, indicating that slip on the glide planes is indeed preferred, in agreement with experiments.

In the following, we present an alternative model to describe this transition in the yield stress and try to relate it to the BDT (Pirouz *et al.* 1999a,b, 2000).

3.1. *Yield behaviour below and above* T_c

As shown in the previous section, our TEM results show that the microstructure of the SiC samples that were deformed below T_c consisted predominantly of only Si(g) leading partials while the microstructure of samples deformed above T_c consisted predominantly of dissociated screw dislocations (leading–trailing pairs). Let us now consider the production of dislocations during deformation of such a tetrahedrally coordinated crystal. In general, the easiest way to produce dislocations in a crystal that contains appropriate sources is by the Frank–Read mechanism. However, if only partial Frank–Read sources are activated at low temperatures (by the operation of the leading partial dislocations only), then such a source will not be a multiplication site for dislocations but can operate only once. Subsequently, the stress will have to be relieved either by fracturing the sample or else by nucleating dislocations from the sample surfaces (or, less likely, within the bulk).

In the energetics of dislocation nucleation, thermal activation is often thought to play a negligible role. The reason for this is thought to be that the available thermal energy kT at a temperature T is too small compared with the large enthalpy barrier ΔH_n required for dislocation nucleation. In terms of the reaction rate theory, thermally activated processes are statistical phenomena whereby atoms that vibrate with a frequency of about ν_0 (10^{13} s^{-1}) have a Boltzmann probability $\exp(-\Delta H_n/kT)$ of overcoming the enthalpy barrier. Accordingly, the frequency ν with which such an activation will occur will be:

$$\nu = \nu_0 \exp\left(-\frac{\Delta H_n}{kT}\right), \tag{7}$$

that is the mean time t, during which a successful activation occurs is $t = (1/\nu_0)\exp(\Delta H_n/kT)$. For dislocation nucleation, the enthalpy barrier ΔH_n is

thought to be so large ($100kT$ or greater) that the time t for a successful operation becomes unreasonably large (e.g. $t \approx 2.7 \times 10^{30}$ s for an activation enthalpy of $100kT$). However, similar to dislocation glide (equation (2)), the free energy for dislocation nucleation is also probably a function of the applied stress. As a first approximation, the variation in the free-energy change ΔG_n (or enthalpy change ΔH_n) with the applied shear stress τ may be assumed to be linear, that is the effective enthalpy barrier ΔH_n^{eff} may be assumed to be reduced by the applied stress τ according to the following equation:

$$\Delta H_n^{eff} \approx \Delta H_n - \alpha\tau V^*. \tag{8}$$

In this equation, $\alpha\tau$ is the stress concentration at a heterogeneity (e.g. a scratch at the surface) and V^* is the activation volume $(= -(\partial H_g/\partial \tau)_T)$. Thus, in the presence of a shear stress, the enthalpy barrier ΔH_n for dislocation nucleation is reduced by an amount $\alpha\tau V^*$ to ΔH_n^{eff}. Accordingly, the probability of overcoming the barrier becomes $\exp[-(\Delta H_n - \alpha\tau V^*)/kT]$ and the frequency of successful dislocation nucleation events will be $\nu = \nu_0 \exp[-(\Delta H_n - \alpha\tau V^*)/kT]$. Hence, the mean time t during which a successful activation occurs will be

$$t = \frac{1}{\nu_0}\exp\left(\frac{\Delta H_n - \alpha\tau V^*}{kT}\right). \tag{9}$$

Based on the experimental results, we shall assume that, in the above equation, the leading and trailing partials have different activation enthalpies for dislocation nucleation, ΔH_n^l and ΔH_n^t respectively, and that $\Delta H_n^l < \Delta H_n^t$. In addition, in equations (8) and (9), the resolved shear stresses on the leading and trailing partial dislocations will be different because they have different Burgers vectors.

Since our experiments were performed on hexagonal SiC, we shall use this material as an example, but the arguments are essentially general and can be applied to other semiconductors. Figure 6(a) shows a schematic diagram of the orientation of the parallelepiped sample used in our compression experiments. The sample is oriented for single glide, that is an orientation in which the $(0001)\langle\bar{2}110\rangle$ slip system is primarily activated. The dislocations most probably nucleate heterogeneously as half-loops from the crystal surface; an example of one (denoted as A) on a particular (0001) slip plane is shown in figure 6(a). For comparison, the nucleation of a dislocation (full-)loop (denoted as A') on the same (0001) slip plane within the sample is also shown. In fact, nucleation of four types of loop on a (0001) slip plane may be envisaged, as illustrated in figure 6(b). In cases A and A', only the leading partial has nucleated while, in cases B and B', nucleation of the leading partial has been followed by that of the trailing partial.

The formation of a dislocation loop presumably takes place by, first, the nucleation of the leading partial, followed by the nucleation of the trailing partial. Assuming that intrinsic faults are favoured over extrinsic faults, then the order of nucleation of the two partials can be determined from the Thomson tetrahedron (Hirth and Lothe 1968). It is important to note that once the leading partial forms, it creates a stacking fault behind it that changes the state of the lattice for nucleation of the trailing partial. The stacking fault of course adds an extra stress term γ/b to the external applied stress that should make it simpler for the trailing partial to nucleate.

It was mentioned above that the assumption has been made that ΔH_n^l and ΔH_n^t are different and that $\Delta H_n^l < \Delta H_n^t$. In fact, there is some independent evidence for this hypothesis in GaSb and GaAs (Ning *et al.* 1995) and also in silicon (Ning and
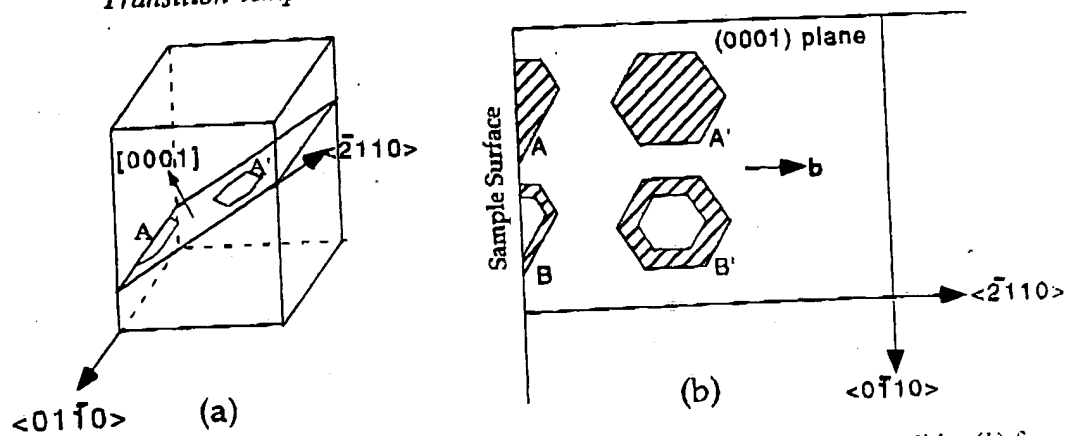
Figure 6. (*a*) The geometry of a deformation sample oriented for single glide; (*b*) four possible ways of dislocation nucleation on the slip plane.

Huvey 1996). There is, however, even more evidence for a related property of the leading and trailing partials in tetrahedrally coordinated crystals: the difference in their mobilities (for the case of silicon and germanium, see for example Wessel and Alexander (1977) and Alexander *et al.* (1980)). It appears that this difference increases as the temperature decreases. Of particular importance is the mobility difference between the two 30° partials of a dissociated screw dislocation where it is found that, even in the elemental semiconductors, silicon and germanium, the leading 30° partial has a higher mobility than the trailing 30° partial. This implies that the activation enthalpies ΔH_g^l and ΔH_g^t for glide of partial dislocations are also different and that $\Delta H_g^l < \Delta H_g^t$. The reasons for the mobility and nucleation differences of the two partials are not really clear, but they probably have a similar origin. One obvious difference is the presence of a stacking fault after the formation of the leading partial that provides a different local environment for nucleation of the trailing partial. However, it is unlikely that the nucleation of a dislocation in a faulted region of the crystal will be significantly different from nucleation in a perfect crystal. Moreover, the presence of a stacking fault provides an extra stress term that should actually help the nucleation of the trailing partial. Another possibility is that the formation (and glide) of the leading partial may result in the creation of point defects in its wake (i.e. in the faulted region) which would have a much more significant effect on the local environment in which the trailing partial is nucleated. These point defects need not of course be extrinsic but can be intrinsic such as jogs or antiphase defects (Hirsch 1980, Heggie and Jones 1983). The interaction of point defects with dislocations and its effect on dislocation mobility goes back to the early work of Celli *et al.* (1963) and Rybin and Orlov (1970) on materials with a high Peierls barrier. Also, in the late 1970s and 1980s, the Soviet scientists performed many experiments on silicon and germanium showing that the region of a crystal swept by a moving dislocation is significantly different from a virgin material, thus affecting the motion of subsequent dislocations (for example Bondarenko *et al.* 1981). Some important evidence comes from the electron spin resonance experiments of Kisielowski-Kemmerich (1990) that revealed the generation of point defects by screw dislocations in silicon. In fact, in his classic review of dislocations in semiconductors, Alexander (1986) emphasizes that a consideration of the dislocation–point-defect interactions is essential to an understanding of the physics of dislocations in these materials. It is also important to realize that the point defects usually annihilate

P. Pirouz *et al.*

(or anneal out) at higher temperatures and their interaction with dislocations becomes less effective.

In the case of compound semiconductors, where the atomistic cores of the leading and trailing partials may be different, the core nature is another factor that must be taken into account in considering dislocation nucleation. Thus, in the case of SiC, the partial with the silicon core may have a smaller activation enthalpy than the partial with the carbon core. As was mentioned before, half of a partial loop (with any Burgers vector) has a silicon-core while the other half has a carbon core (figure 1). We suggest that, in the case of SiC, the Si(g) half-loop of the leading partial (whose Burgers vector is determined from the Thomson tetrahedron) is preferentially nucleated compared with a completely C(g) or a mixed Si(g)–C(g) half-loop (figure 7(a)).

Assuming that, at $T < T_c$, only the leading Si(g) partial (Burgers vector $\mathbf{b}_1$) is nucleated, then the sequence of events is illustrated in figure 7. After its nucleation from the sample surface (figure 7(a)), the half-loop expands and, because of the different mobilities of the segments, the semihexagonal shape of the half-loop is distorted. Assuming that the 90° Si(g) partial has a higher mobility than the two adjoining 30° partials, the configuration of the half loop at a later stage becomes something like that shown in figure 7(b). In figure 7(c), the 90° partial has moved out of the specimen and the lower 30° segment (which has been assumed to be more mobile than the upper 30° segment) is in the process of moving out. The final outcome will be a preponderance of 30° Si(g) dislocations left on different (and parallel) (0001) planes. Note that only a few partials can exist on each particular (0001) plane (figure 6(b)) because each partial drags a stacking fault behind it and the initial source (AD in figure 7(a)) is deactivated as a dislocation source.

Now consider the nucleation of a perfect dislocation half-loop from the sample surface (B in figure 6(b)) at $T > T_c$. The atomistic detail of the half-loop B in figure 6(b) is shown in figure 8 where the cores of all the half-loop segments are shown reconstructed. The sequence of events after nucleation, that is the expansion of the perfect dislocation half-loop on the (0001) slip plane, is illustrated in figure 9. Here, a dissociated dislocation half-loop, ABCD, nucleates from the surface (figure 9(a)) and expands (figure 9(b)) until the mobile segments run out of the sample (figure 9(c)), leaving only the slow dissociated screw dislocation on the (0001) slip planes. In this figure, additional assumptions have been made that mobility of the upper 90°Si(g)–30°Si(g) segment is higher than that of the lower 30°Si(g)–90°Si(g) segment, which in turn is higher than the topmost 30°Si(g)–30°C(g) screw segment. The final configuration will be a preponderance of 30°Si(g)–30°C(g) screw dislocations parallel

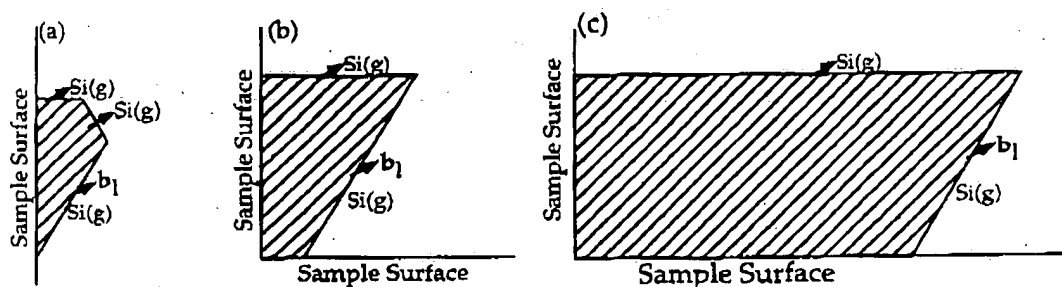Figure 7. Nucleation and expansion of a leading partial dislocation half-loop from the surface of the crystal at $T < T_c$.
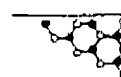
to the $[\bar{2}110]$ direction in the deformed crystal. Clearly, a better knowledge of the partial mobilities is essential to draw clearer conclusions. Multiplication of dislocations from, say, Frank–Read sources is probably much easier than their nucleation. Thus, as soon as the density of (perfect) dislocations in the crystal exceeds about 10^3–$10^4\,cm^{-2}$, presumably multiplication, rather than nucleation, will take over as the dominant mechanism of increasing the dislocation density for deformations above T_c.

3.2. *Relation between T_c and T_{BDT}*

The next problem to consider is the possible relation between the transition in the $\tau_Y(T)$ plot and the BDT temperature. When a load is applied to a crystal, it is initially deformed elastically whereby elastic energy is stored in the crystal. This stored elastic energy is released if the load is taken off. If, however, loading is continued, at a rate $\dot{\tau}$, and the stored energy continuously increases, there are two main competing ways for the crystal to relax and decrease its overall elastic energy. One way is by brittle fracture of the crystal whereby the energy is consumed in creating two new surfaces as a crack forms and propagates.

The second way for the release of the stored elastic energy is to move pre-existing dislocations or to nucleate and move fresh (as well as pre-existing) dislocations. The occurrence of brittle fracture versus plastic yielding of a crystal is determined by the competition between these two ways of releasing the stored elastic energy. In the case of crack propagation, the Griffith criterion can be written in the form

$$\frac{(1 - \nu^2)K_{eff}^2}{E} \geqslant 2\gamma_s, \tag{10}$$

where ν is Poisson's ratio, E is the elastic modulus, γ_s is the surface energy and K_{eff} is the effective stress intensity factor given by (Thomson 1986)

$$K_{eff} = K_{app} - K_d \tag{11}$$

with

$$K_{app} = (\pi a)^{1/2}\sigma_{app}, \tag{12}$$
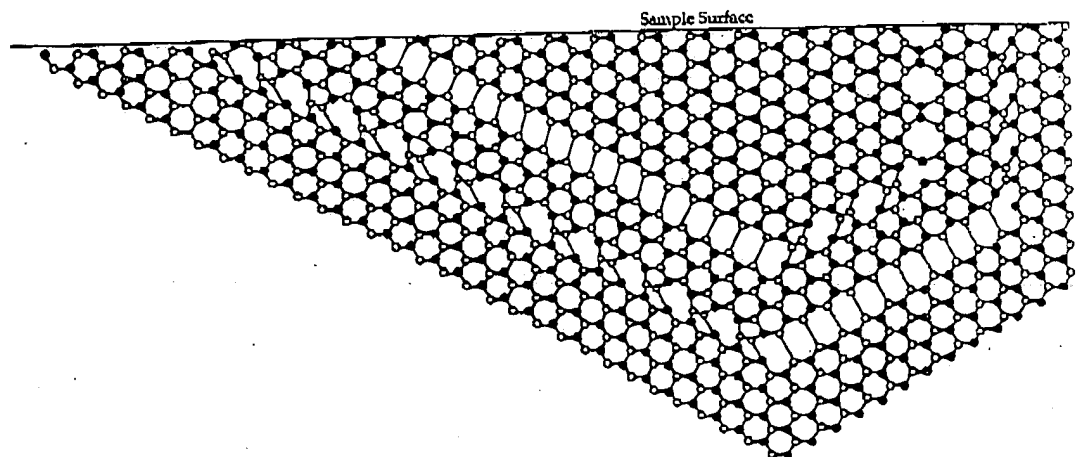
Figure 8.   Schematic illustration of the atomistic detail of a dissociated (leading–trailing) dislocation half-loop nucleated from the surface of the crystal at $T > T_c$.
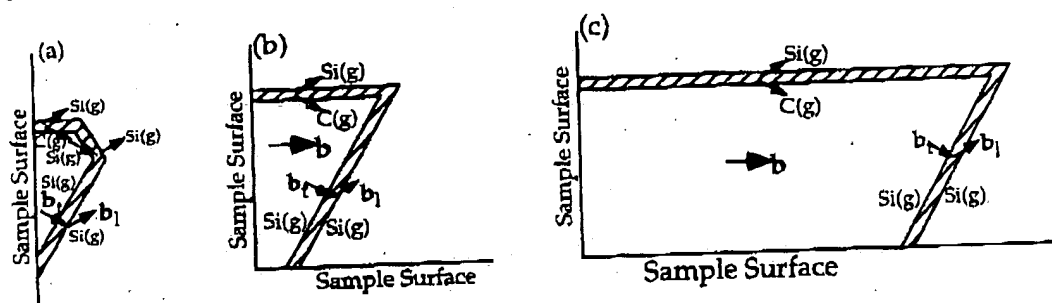
P. Pirouz *et al.*

Figure 9. Nucleation and expansion of a dissociated (leading–trailing) dislocation half-loop from the surface of the crystal at $T > T_c$.

σ_{app} being the applied tensile stress and a the crack half-length. K_d in equation (11) is the shielding of the crack tip introduced by the compressive stress of the dislocations around it; this results in a reduction of the applied tensile stress on the crack tip.

In the above conventional picture, brittleness versus ductility of a loaded crystal is considered as the competition between shearing of the crystal by dislocation motion and rupture of the bonds at the tip of a microcrack within the crystal. The general view is that the stress needed for plastic yielding (i.e. the yield stress τ_Y) is strongly temperature dependent and decreases rapidly with increasing temperature while the (tensile) stress required for fracturing the bonds σ_F (and the corresponding shear stress τ_F) has a much weaker temperature dependence (Kelly *et al.* 1967). As a result, $\tau_F(T)$ and $\tau_Y(T)$ intersect at a critical temperature T_{BDT}, usually known as the BDT temperature, where $\tau_F < \tau_Y$ at $T < T_{BDT}$ (the brittle regime) and $\tau_Y < \tau_F$ at $T > T_{BDT}$ (the ductile regime).

In the model described in this paper (as illustrated in figure 10) the BDT, at least in tetrahedrally coordinated materials, is determined by the competition between the nucleation and propagation of leading partial dislocations versus the nucleation and propagation of perfect (total) dislocations (i.e. that of the trailing partial) As shown by equation (9), the nucleation and propagation of dislocations (partial or perfect) are temperature and stress dependent. Thus, the rupture of atomic bonds enters the picture only indirectly. It is argued that, in a constant-strain-rate experiment, if the temperature and stress are not sufficient to nucleate the trailing partial (and thus the
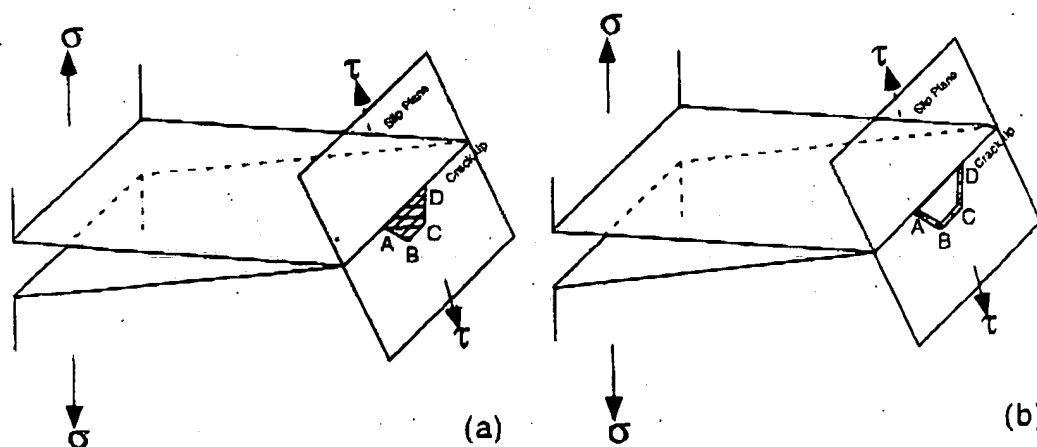

Figure 10. Schematic illustration of dislocation nucleation at a crack tip under mode I loading: (*a*) at $T < T_c$; (*b*) at $T > T_c$.

perfect) dislocations, then the increasing stress will eventually reach a sufficient value σ_F to rupture the bonds at the crack tip, leading to its propagation. In such a regime, leading partial dislocations may well nucleate at the crack tip (as well as in other favourable sites) but, if at any particular site, the leading partial is not followed by nucleation of the trailing partial, then the source will shut off and stop operating. The consequence is that dislocation nucleation will soon stop and plastic deformation is limited to the strain produced by the few partial dislocations generated before the sources stopped operating. Meanwhile, the work done on the crystal by the external load continues to increase the elastic strain energy until the critical strain energy release rate is reached and the crystal gives in and fractures. In this way, the details of bond rupture at the crack tip or temperature dependence of σ_F (or τ_F) are irrelevant to the problem of the BDT.

What is of primary importance in the present model is the temperature dependence of τ_n^l and τ_n^t, the minimum shear stresses required to nucleate the leading and the trailing (i.e. the total) dislocation respectively. The BDT temperature is given by the intersection of $\tau_n^l(T)$ and $\tau_n^t(T)$ plots. Now, when an increasing K (related to the shear stress τ by $K = \beta^{-1}\tau$, where β is a geometrical factor) is applied at a rate of $\dot{K}$, the question to be asked is whether a successful (dislocation) nucleation event will occur during the time period in which K increases from its initial value K_0 to the stress intensity factor K_{Ic} at which the crystal fails (figure 11). Note that, as K (i.e. τ) increases, the effective activation enthalpy for dislocation nucleation decreases. Thus, the BDT is determined by a competition between the first occurrence of two events: either K reaches K_{Ic} first and catastrophic failure occurs, or $\Delta H_n^t - \alpha\beta KV^*$ decreases sufficiently to result in the nucleation of the (trailing partial) dislocation. The time taken for K to reach K_{Ic} is $(K_{Ic} - K_0)/\dot{K}$ (figure 11). Thus, the condition for BDT is that

$$t \leqslant \frac{K_{Ic} - K_0}{\dot{K}}.$$

Let the stress intensity factor reach a value $K = K_Y$ at T_{BDT} to nucleate dislocations. Thus $t = (K_Y - K_0)/\dot{K}$, giving
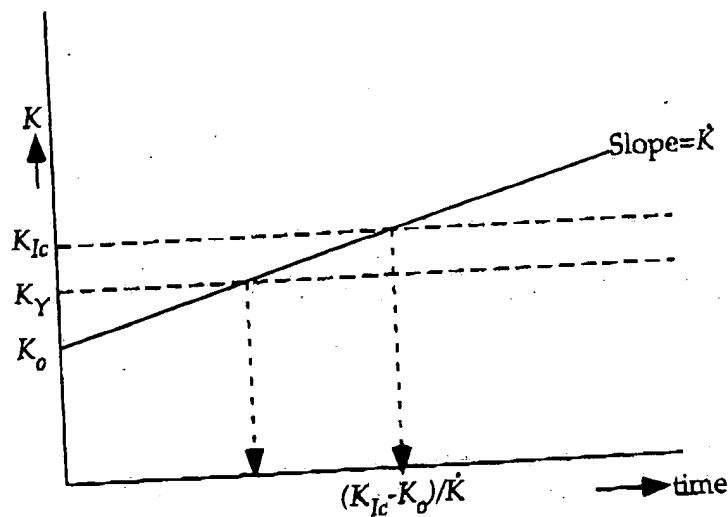

Figure 11.   Schematic plot of K versus time in a constant-$\dot{K}$ experiment.

1224

P. Pirouz *et al.*

$$\frac{1}{\nu_0}\exp\left(\frac{\Delta H_h^t - \alpha\tau_Y V^*}{kT_{BDT}}\right) = \frac{K_Y - K_0}{\dot{K}},$$

that is

$$\dot{K} = \nu_0(K_Y - K_0)\exp\left(-\frac{\Delta H_n^t - \delta K_Y}{kT_{BDT}}\right), \qquad (13)$$

where $\delta = \alpha\beta V^*$ is a constant. Thus, a plot of $\ln(\dot{K})$ versus $1/T_{BDT}$ should be a straight line with a slope $(\Delta H_n^t - \delta K_Y)/k$ and an intercept $\ln[\nu_0(K_Y - K_0)]$. Since experiments show that a plot of $\ln(\dot{K})$ versus $1/T_{BDT}$ has a slope equal to that of (total) dislocation glide velocity (for example St John 1975, Behrensmeier *et al.* 1987, Brede and Haasen 1988, Samuels and Roberts 1989, Brede 1993), then equation (12) implies that the activation enthalpy for nucleation of the trailing partial dislocation, given by $\Delta H_n^{eff} = \Delta H_n^t - \delta K_Y$, is approximately the same as that for dislocation glide. Assuming for the moment that T_c is indeed identical with T_{BDT}, then one can obtain a first estimate of the activation enthalpy from the values of T_c at the two strain rates obtained in the experiment described in this paper. Since $T_c \approx 1100°C$ at $\dot{\varepsilon} \approx 3.6 \times 10^{-5}\,s^{-1}$ and $T_v \approx 1030°C$ at $\dot{\varepsilon} \approx 2.6 \times 10^{-6}\,s^{-1}$, one obtains

$$\frac{\ln(3.6 \times 10^{-5}/2.6 \times 10^{-6})}{(1/1373 - 1/1303)} = -67165\,K,$$

giving an activation enthalpy of about 5.8 eV. Although this is higher than $\Delta H_g \approx (4.5-5.1) \pm 0.3\,eV$ for activation enthalpy of (perfect) dislocation glide in 4H-SiC (obtained from the slope of the high-temperature region of the $\ln(\tau)$ versus $1/T$ plots in figures 2 (*a*) and (*b*)), it is not too bad as a first approximation. Further experiments are planned to obtain the shift of T_c at other strain rates, and to see whether a plot of $\ln(\dot{K})$ versus $1/T_c$ is indeed linear. If so, a better value of the activation energy can be obtained from the slope of the linear plot and compared with ΔH_g. Similar experiments on other semiconductors would also be highly desirable.

3.3. Incidence of perfect (or narrowly dissociated) screw dislocations during very-low temperature ($T \ll T_c$) deformations

A number of experiments have shown that when high-quality (very-low-dislocation-density) semiconducting crystals are deformed under hydrostatic pressure, there is a range of temperatures $T_{BDT} > T > T_{II}$, over which the crystal is extremely brittle (Suzuki *et al.* 1999a,b, Edagawa *et al.* 2000). This is so much so that, if the crystals have not already fractured during the deformation test, then they usually shatter into small pieces during decompression of the sample cell. An example is GaAs that was found to be extremely brittle between 300 and 400 K even when the confining pressure was increased up to 1.2 GPa; consequently, it has been very difficult to prepare thin foils and to perform TEM experiments on the samples deformed in this range (Suzuki *et al.* 1999a). However, interestingly, below this range, that is at temperatures less than T_{II}, it again becomes possible to deform the crystal, albeit at very high stresses and under hydrostatic pressure. Thus, Suzuki *et al.* (1999a) could deform GaAs at 300 K under a confining pressure of 400 MPa! TEM of samples deformed at these very low temperatures show a microstructure consisting of predominantly *perfect* screw dislocations. At first sight, this appears to be contrary to the argument

put forward in this paper that only leading partial dislocations may be nucleated at $T < T_{\mathrm{BDT}}$. However, according to equation (8), the effective activation enthalpy for dislocation nucleation, given by $\Delta H_n^{\mathrm{eff}} = \Delta H_n - \alpha\tau V^*$, is lowered by the applied resolved shear stress τ. Thus, it may be that the very high stresses (over 0.5 GPa) applied at temperatures below T_{II}, lower the activation enthalpy sufficiently to make nucleation of the trailing partial dislocation possible, resulting in leading–trailing pairs of partials, that is perfect dislocation half-loops. This is also supported by theoretical calculations of Brochard *et al.* (1998) who have shown that the nucleation of dislocations is stress dependent and, at sufficiently high applied stresses, both partials can nucleate from a surface source. It is also possible that, at moderately low temperatures ($T < T_{\mathrm{II}}$), partial dislocations are nucleated sequentially (leading followed by trailing) on the glide plane but at very low temperatures ($T \ll T_{\mathrm{II}}$), where the shear stress required to nucleate dislocations becomes very high, it becomes energetically favourable for perfect *undissociated* dislocations to nucleate and propagate on the shuffle plane, as suggested by Duesbery. The screw nature of the dislocations is probably due to the much higher velocity of non-screw segments of a half-loop which, under the very high stresses, rapidly move out of the crystal and leave the much slower screw segments in the sample (as in figure 9).

§4. CONCLUSION

New deformation experiments on 4H-SiC confirm the existence of a transition temperature in the critical yield stress that is close to the BDT of this material. Similar to the lowering of the BDT temperature, the critical temperature T_c in the variation in the yield stress with temperature is also lowered with decreasing strain rates. The decrease in T_c is about 70°C from 1100°C at $\dot{\varepsilon} = 3.6 \times 10^{-5}\,\mathrm{s}^{-1}$ to 1030°C at $\dot{\varepsilon} = 2.6 \times 10^{-6}\,\mathrm{s}^{-1}$. TEM experiments have verified that the low density of dislocations produced in the samples deformed below T_c are predominantly single leading partials with a silicon core, while a high density of Si(g)–C(g) dissociated screw dislocations are produced in the samples deformed above T_c. A model has been presented that associates the transition temperature T_c with a change in the mode of deformation. In this model, only leading partial dislocations are nucleated at $T < T_c$, which glide on parallel slip planes but contribute to a very limited extent to the straining of the crystal, especially since the sources that produced them become inoperative after they emit only one partial dislocation. On the other hand, at $T > T_c$, full dislocations can be nucleated repeatedly from sources in the crystal and their glide produces large strains and causes macroscopic yielding of the crystal. Additionally, the model relates the transition temperature T_c in the yielding of the crystal to the temperature at which the BDT in the fracture of the crystal occurs. The formation of perfect screw dislocations at very low temperatures in semiconductors is attributed to the very high applied stresses that lower the activation enthalpy for the nucleation of the trailing partial dislocations. Deformation experiments in the brittle regime of various semiconductors, both at moderately low and very low temperatures, combined with TEM characterization of the resulting dislocation configurations, will be very valuable to shed more light on the mode of dislocation nucleation and the transition in fracture mode of these materials.

1226   P. Pirouz *et al.*

REFERENCES

ALEXANDER, H., 1986, *Dislocations in Solids*, Vol. 7, edited by F. R. N. Nabarro (Amsterdam:
    Elsevier), pp. 114–234.
ALEXANDER, H., EPPENSTEIN, H., GOTTSCHALK, H., and WENDLER, S., 1980, *J. Microsc.* **118**,
    13.
ALEXANDER, H., HAASEN, P., LABUSCH, R., and SCHRÖTER, W., 1979, *J. Phys. Paris*, **40**, C6
    (Foreword).
ALEXANDER, H., and HAASEN, P., 1968, *Solid St. Phys.*, **22**, 27.
BEHRENSMEIER, R., BREDE, M., and HAASEN, P., 1987, *Scripta Metall.*, **21**, 1581.
BONDARENKO, I. E., EREMENKO, V. G., FARBER, B. Y., NIKITENKO, V. I., and YAKIMOV, E.
    B., 1981, *Phys. Stat. sol.* (b), **68**, 53.
BREDE, M., 1993, *Acta metall. mater.*, **41**, 211.
BREDE M., and AND HAASEN, P., 1988, *Acta metall.*, **36**, 2003.
BROCHARD, S., RABIER, J., and GRILHE, J., 1998, *Eur. Phys. J.*, **2**, 99.
CASTAING, J., VEYSSIÈRE, P., KUBIN, L. P., and RABIER, J., 1981, *Phil. Mag. A*, **44**, 1407.
CELLI, V., KABLER, M., NINOMIYA, T., and THOMSON, R., 1963, *Phys. Rev.*, **131**, 58.
CHERNS, D., and PRESTON, A. R., 1986, *Proceedings of the 11th International Congress on
    Electron Microscopy*, edited by T. Imura, S. Marusa and T. Suzuki (Kyoto: Japan
    Society of Electron Microscopy), p. 721.
CHIAO, Y.-H., and CLARKE, D. R., 1989, *Acta metall.*, **37**, 203.
CHOU, C. T., PRESTON, A. R., and STEEDS, J. W., 1992, *Phil. Mag. A*, **65**, 863–888.
CORMAN, G. S., 1992, *J. Am. Ceram. Soc.*, **75**, 3421.
DEMENET, J. L., 1987, Thèse d'Etat 457, Université de Poitiers (UFR Sciences Fondamentales
    et Appliquéees).
DEMENET, J. L., BOIVIN, P., and RABIER, J., 1989, *Proceedings of the International Symposium
    on Structure and Properties of Dislocations in Semiconductors*, edited by S. G. Roberts,
    D. B. Holt and P. R. Wilshaw (Bristol: Institute of Physics), pp. 415–420.
DEMENET, J.-L., HONG, M. H., and PIROUZ, P., 2000, *Scripta mater.*, **43**, 865.
DUESBERY, M. S., and JOÓS, B., 1996, *Phil. Mag. Lett.*, **74**, 253.
DUESBERY, M. S., and RICHARDSON, G. Y., 1991, *Solid St. Mater. Sci.*, **17**, 1.
EDAGAWA K., KOIZUMI, H., KAMIMURA, Y., and SUZUKI, T., 2000, *Phil. Mag. A*, **80**, 2591.
FUJITA, S., MAEDA, K., and HYODO, S., 1987, *Phil. Mag. A*, **55**, 203.
GEORGE, A., 1998, *Solid St. Phenom.*, **59–60**, 251.
GEORGE, A., and MICHOT, G., 1993, *Mater. Sci. Engng.* A164, 118.
GEORGE, A., and RABIER, J., 1987, *Rev. Phys. Appl.*, **22**, 941.
GILMAN, J. J., 1960, *J. appl. Phys.*, **31**, 2208.
GOTTSCHALK, H., PATZER, G., and ALEXANDER, H., 1978, *Phys. Stat. sol.* (a), **45**, 207.
HAASEN, P., BREDE, M., and ZHANG, T., 1989, *Proceedings of the International Symposium on
    Structure and Properties of Dislocations in Semiconductors*, edited by S. G. Roberts, D.
    B. Holt and P. R. Wilshaw (Bristol: Institute of Physics), pp. 361–372.
HANSEN, L. B., STOKBRO, K., LUNDQVIST, B. I., JACOBSEN, K. W., and DEAVEN, D. M., 1995,
    Phys. Rev. Lett., **75**, 4444.
HEGGIE, M., and JONES, R., 1983, *Phil. Mag. B*, **48**, 365.
HIRSCH, P. B., 1980, *J. Microsc.*, **118**, 3.
HIRSCH, P. B., PIROUZ, P., ROBERTS, S. G., and WARREN, P. D., 1985, *Phil. Mag. B*, **52**, 759.
HIRSCH, P. B., and ROBERTS, S. G., 1991, *Phil. Mag. A*, **64**, 55; 1996a, *Acta mater.*, **44**, 2361;
    1996b, *Scripta mater.*, **35**, 291; 1997, *Phil. Trans. R. Soc.*, **355**, 1991.
HIRSCH, P. B., ROBERTS, S. G., and SAMUELS, J., 1989a, *Proc. R. Soc. A*, **421**, 25.
HIRSCH, P. B., ROBERTS, S. G., SAMUELS, J., and WARREN, P. D., 1989b, *Proceedings of the
    International Symposium on the Structure and Properties of Dislocations in Semicon-
    ductors*, edited by S. G. Roberts, D. B. Holt and P. R. Wilshaw (Bristol: Institute of
    Physics), pp. 373–384.

HIRTH, J. P., and LOTHE, J., 1968, *Theory of Dislocations* (New York: McGraw-Hill).

HSIAH, K. J., and ARGON, A. S., 1994, *Mater. Sci. Engng.* **A164**, 111.

JOÓS, B., REN, Q., and DUESBERY, M. S., 1994, *Phys. Rev. B*, **50**, 5890.

KAXIRAS, E., and DUESBERY, M. S., 1993, *Phys. Rev. Lett.*, **70**, 3752.

KELLY, A., TYSON, W. R., and COTTRELL, A. H., 1967, *Phil. Mag.*, **15**, 567.

KHANTA, M., 1994, *Scripta metall. Mater.*, **31**, 1355.

KHANTA, M., POPE, D. P., and VITEK, V., 1994a, *Scripta metall. Mater.*, **31**, 1349; 1994b, *Phys. Rev. Lett.*, **73**, 684.

KHANTA, M., and VITEK, V., 1996, *Scripta mater.*, **35**, 285.

KISIELOWSKI-KEMMERICH, C., 1990, *Phys. Stat. sol.* (b), **161**, 111.

KOCKS, U. F., ARGON, A., and ASHBY, M. F., 1975, *Prog. Mater. Sci.*, **19**, 1.

KOSTERLITZ, J. M., and THOULESS, D. J., 1973, *J. Phys. C*, **6**, 1181.

KUBIN, L. P., 1974, *Phil. Mag.*, **30**, 705.

MAEDA, K., and FUJITA, S., 1989, *Lattice Defects in Ceramics*, edited by S. Takeuchi and T. Suzuki (Tokyo), pp. 25–31.

MICHOT, G., 1988, *Cryst. properties and Preparation*, **17–18**, 55.

MICHOT, G., and GEORGE, A., 1982, *Scripta metall.*, **16**, 519; 1986, *ibid.*, **20**, 1495; 1989, *Proceedings of the International Symposium on Structure and Properties of Dislocations in Semiconductors*. edited by S. G. Roberts, D. B. Holt and P. R. Wilshaw (Bristol: Institute of Physics), pp. 385–396.

MICHOT, G., GEORGE, A., CHABLI-BRENAC, A., and MOLVA, E., 1988, *Scripta metall.*, **22**, 1043.

NING, X. J., and HUVEY, N., 1996, *Phil. Mag. Lett.*, **74**, 241.

NING, X. J., PEREZ, T., and PIROUZ, P. 1995, *Phil. Mag. A*, **72**, 837.

NING, X. J., and PIROUZ, P., 1996, *J. Mater. Res.*, **11**, 884.

PIROUZ, P., KUBIN, L. P., DEMENET, J. L., HONG, M. H., and SAMANT, A., 2000, *Proceedings of the Symposium on Multiscale Phenomena in Materials Experiments and Modeling*, Materials Research Society Symposium Proceedings, Vol. 578, edited by I. M. Robertson, D. H. Lassila, B. Devincre and R. Phillips (Pittsburgh, Pennsylvania: Materials Research Society), pp. 205–216.

PIROUZ, P., and NING, X. J., 1995, *Proceedings of the Conference on the Microscopy of Semiconducting Materials*, edited by A. G. Cullis and A. Staton-Bevan (Bristol: Institute of Physics), pp. 69–77.

PIROUZ, P., SAMANT, A. V., HONG, M. H., MOULIN, A., and KUBIN, L. P., 1999a, *J. Mater. Res.*, **14**, 2783; 1999b, *Proceedings of the Conference on the Microscopy of Semiconducting Materials*, edited by A. G. Cullis and R. Beanland, Institute of Physics Conference Series, Vol. 164 (Bristol: Institute of Physics), pp. 61–66.

RABIER, J., GAREM, H., DEMENET, J. L., and VEYSSIÈRE, P., 1985, *Phil. Mag. A.* **51**, L67.

RABIER, J., and GEORGE, A., 1987, *Rev. Phys. Appl.*, **22**, 1327.

REN, Q., JOÓS, B., and DUESBERY, M. S., 1995, *Phys. Rev. B*, **52**, 13 223.

RYBIN V. V., and ORLOV, A. N., 1970, *Soviet Phys. Solid St.*, **11**, 2635.

SAMANT, A. V., 1999, PhD Thesis, Case Western Reserve University,

SAMANT, A. V., and PIROUZ, P., 1998, *Int. J. Refractory Metals Hard Mater.*, **16**, 277.

SAMANT, A. V., ZHOU, W. L., and PIROUZ, P., 1998, *Phys. Stat. sol* (a), **166**, 155.

SAMUELS, J., and ROBERTS, S. G., 1989, *Proc. R. Soc. A*, **421**, 1.

ST JOHN, C., 1975, *Phil. Mag.*, **32**, 1193.

SERBENA, F. C., and ROBERTS, S. G., 1994, *Acta metall. Mater.*, **42**, 2505.

STILLINGER, F. H., and WEBER, T. A., 1985, *Phys. Rev. B*, **31**, 5262.

SUN, Y.-Q., HAZZLEDINE, P. M., and DIMIDUK, D. M., 1998, *Phase Transformations and Systems Driven Far From Equilibrium*, edited by E. Ma, P. Bellon, M. Atzmon and R. Trivedi (Pittsburgh, Pennsylvania: Materials Research Society), pp. 261–266.

SUZUKI, T., NISHISAKO, T., TARU, T., and YASUTOMI, T., 1998, *Phil. Mag. Lett.*, **77**, 173–180.

SUZUKI, T., YASUTOMI, T., TOKUOKA, T., and YONENAGA, I., 1999a, *Phil. Mag. A*, **79**, 2637; 1999b, *Phys. Stat. sol.* (a), **171**, 47.

TAKEUCHI, S., and SUZUKI, K., 1999, *Phys. St. sol.* (a), **171**, 99.

TAKEUCHI, S., SUZUKI, K., MAEDA, K., and IWANAGA, H., 1984, *Phil. Mag. A*, **50**, 171.

THOMSON, R., 1986, *Solid St. Phys.*, **39**, 1.

WESSEL, K., and ALEXANDER, H., 1977, *Phil. Mag.*, **35**, 1523.